PCCP

View Online
Dynamic Article Links

Cite this: *Phys. Chem. Chem. Phys.*, 2011, **13**, 16437–16443

www.rsc.org/pccp

PAPER

Hydrogen electrocatalysis on overlayers of rhodium over gold and palladium substrates—more active than platinum?

G. Soldano,[a] E. N. Schulz,[b] D. R. Salinas,[b] E. Santos*[ac] and W. Schmickler*[a]

Received 15th May 2011, Accepted 1st August 2011
DOI: 10.1039/c1cp21565e

We have investigated the stability and catalytic activity of epitaxial overlayers of rhodium on Au(111) and Pd(111). Both surfaces show a strong affinity for hydrogen. We have calculated the energy of adsorption both for a strongly and a more weakly adsorbed species; the latter is the intermediate in the hydrogen evolution reaction. Both the energy of activation for hydrogen adsorption (Volmer reaction) and hydrogen recombination (Tafel reaction) are very low, suggesting that these overlayers are excellent catalysts.

1 Introduction

In the search for good and cheap electrocatalysts, much attention has recently been focused on overlayers of metals on a foreign metal substrate. Pseudomorphic overlayers are strained when their lattice constants differ from that of the substrate; the resulting changes in the *d* band structure can significantly modify the catalytic properties of the layer. In addition, there can be a strong chemical, or ligand, effect of the substrate on the adsorbate.[1] This combination can result in good catalytic activity, and is also an excellent field to study the relation between the structure and reactivity of metals.[2–5]

In electrochemistry palladium monolayers on various substrates have been particularly popular, ever since Pd/Au(111) has been shown to be a good catalyst for hydrogen evolution.[4–7] Here we shall investigate theoretically layers of rhodium on Au(111) and Pd(111) and show, that they promise to be even better catalysts for this reaction. The formation of these layers has been well investigated experimentally, but so far there have been no kinetic studies. Thus, we make a prediction for their catalytic properties.

Rhodium on Au(111) grows epitaxially until the second overlayer, afterwards it undergoes cluster growth.[8] We have not found any studies of Rh/Pd(111), but the related system Rh/Pt(111) has been well investigated: Rhodium deposition on Pt(111) is epitaxial until more than five Rh overlayers have been formed.[9–12] Hydrogen interaction with pure rhodium surfaces has been the topic of several experimental investigations conducted in ultrahigh vacuum. Its adsorption has been studied by high resolution electron energy loss spectra,[13] and its diffusion with laser-induced thermal desorption.[14] Hydrogen chemisorption on pure Rh has also been studied theoretically,[15] but to our knowledge, not on rhodium overlayers.

In the present work we first examine the stability of Rh/Au(111) and Rh/Pd(111) layers by density-functional theory (DFT). Next, we shall study hydrogen adsorption, which plays an important role in hydrogen evolution, on various sites. Most articles on hydrogen adsorption consider only the most stable species. However, on transition metal surfaces this species is often only a spectator,[21] while the reaction passes *via* more weakly adsorbed atoms. Therefore, we shall distinguish between strongly adsorbed H_s and weakly adsorbed H_w hydrogen. Since the former often adsorbs at potentials above the equilibrium potential for hydrogen evolution, it is sometimes denoted as hydrogen adsorbed at underpotentials H_{upd},[20] while the other form, H_{opd}, is said to form at overpotentials. However, we prefer not to use this terminology, which is incomprehensible to nonelectrochemists. Finally, we shall investigate the kinetics of hydrogen evolution on these surfaces, using a theory developed in our group.[22,23] The computational details are given in the appendix.

2 Results and discussions

2.1 Stability of Rh/Au(111) and Rh/Pd(111) overlayers

When a monolayer of one metal is deposited epitaxially on another metal substrate with a different lattice constant, a strained overlayer results. Such overlayers can be stable if the inter-metal bonds are stronger than those of the pure metals, and in some cases even epitaxial multilayers can be formed. In order to investigate the stability of rhodium layers on Pd(111) and Au(111) the total and the differential binding energies (E_{bin} and dE_{bin} respectively) have been calculated:

$$E_{bin} = E_{Rh(N)/Sub} - NE_{Rh(bulk)} - E_{Sub} \quad (1)$$

$$dE_{bin} = E_{Rh(N)/Sub} - E_{Rh(bulk)} - E_{Rh(N-1)/Sub} \quad (2)$$

[a] *Institute of Theoretical Chemistry, Ulm University, D-89069 Ulm, Germany. E-mail: esantos@uni-ulm.de, wolfgang.schmickler@uni-ulm.de*
[b] *Instituto de Ingeniería Electroquímica y Corrosión, Universidad Nacional del Sur, Bahía Blanca, Argentina*
[c] *Facultad de Matemáticas, Astronomía y Física, IFEG-CONICET, Universidad Nacional de Córdoba, Argentina*

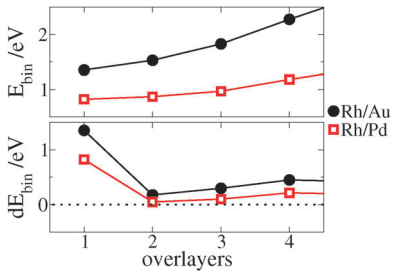

Fig. 1 Total and differential binding energies (E_{bin} and dE_{bin} per atom respectively) of Rh/Pd and Rh/Au multilayers.

where $E_{Rh(N)/Sub}$ is the energy of N layers of Rh on the substrate, $E_{Rh(bulk)}$ is the energy of the Rh bulk per atom (with its own lattice constant), and E_{Sub} is the energy of a pure substrate slab. In the thermodynamic limit, the condition $E_{bin} < 0$ corresponds to the familiar condition $\gamma_s > \gamma_a + \gamma_i$[16] for layer by layer growth, that the surface energy γ_s of the substrate should be larger than the sum of the surface energy γ_a of the adsorbate and the interfacial energy γ_i between the two metals. The surface energy of Rh(111) (2.47 J m^{-2}) is large compared to that of Au(111) (1.28 J m^{-2}),[17] and the lattice constant of Rh is expanded by 8% over Au, so we expect E_{bin} to be positive, and this is indeed the case—see Fig. 1. This is in line with the experimental observation, that in the vacuum Rh on Au(111) shows Volmer–Weber cluster growth.[18] In contrast, in an aqueous electrolyte the first two layers of Rh on Au(111) grow epitaxially and are stable.[8] Obviously, the Rh layers are stabilized by the electrolyte. Water adsorption is particularly strong on Rh(111)— −0.42 eV per water molecule, compared to −0.13 eV on Au(111)[19] and certainly favours layer by layer growth; in addition, specific adsorption might further stabilize the layers. It is difficult to tell if these layers are absolutely stable or only metastable. In any case, experimentally they are stable, and hydrogen evolution proceeds rapidly.[8]

The surface energy of Pd(111) is 1.92 J m^{-2} and thus in between those of Rh(111) and Au(111).[17] In addition, the lattice mismatch between Rh and Pd is only 4%, so we expect monolayers of Rh over Pd(111) to be substantially more stable than Rh/Au(111), and this is indeed the case—see Fig. 1. Nevertheless, our calculations predict cluster growth in the vacuum. There seem to be no experimental data, but the same mechanisms that stabilize Rh/Au(111) in aqueous solutions should also operate for Rh/Pd(111).

To shed some light on the possible metastability of such films we investigated the energetics of nucleation by comparing the energies of a four atom island and a four atom cluster (see Fig. 2).

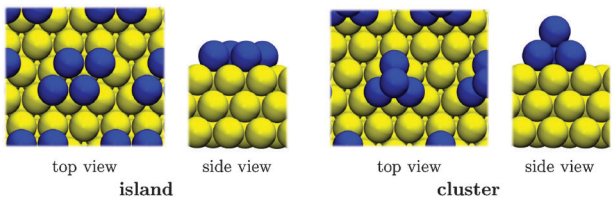

Fig. 2 Top and side views of four atom islands and clusters on Au(111) and Pd(111) substrates.

In both cases, the energies of the islands are more favourable than those of the clusters: by −0.09 eV for Rh/Au, and by −0.64 eV for Rh/Pd(111). So at least for small clusters there is a kinetic barrier for the formation of cluster; in electrochemical systems this barrier would be enhanced by the presence of water, which interacts more strongly with Rh than with Au or Pd, and thus favours island growth.

2.2 Hydrogen adsorption on Rh(111) surfaces

Adsorbed hydrogen is the intermediate in hydrogen evolution and oxidation, and its energetics have a pronounced influence on the reaction rate. As mentioned in the introduction, on transition metals the first hydrogen atoms are often adsorbed so strongly that they are difficult to desorb in the second step, and hence act like a spectator. Therefore, we have considered two types of hydrogen, a strongly H_s and a weakly H_w adsorbed species; their adsorption sites on Rh(111) are illustrated in Fig. 3. The adsorption energies are obtained from:

$$E^{s}_{ads} = [E(H_s/Sub) - E(Sub)]/n - \frac{E(H_2)}{2} \qquad (3)$$

$$E^{w}_{ads} = E(H_w/H_s/Sub) - E(H_s/Sub) - \frac{E(H_2)}{2} \qquad (4)$$

where n is the number of adsorbed atoms per unit cell, $E(H_s/Sub)$ is the energy of a Rh(111) substrate fully covered with H_s, $E(H_w/H_s/Sub)$ is the energy of H_w adsorbed on the latter, $E(Subs)$ and $E(H_2)$ are the energies of the clean substrate and of the hydrogen molecule in vacuum respectively. The adsorption energies for coverages of 1 and 0.25 monolayers (ML) are shown in Fig. 4.

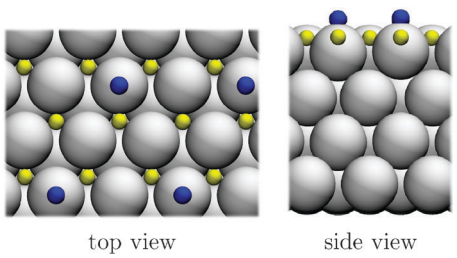

Fig. 3 Top and side view of the strongly adsorbed hydrogen H_s (yellow) and the weakly adsorbed hydrogen H_w (blue) on Rh(111). H_s is adsorbed on the fcc hollow site, H_w on the top. The diagram is for a full monolayer of H_s and a coverage of 1/4 for H_w.

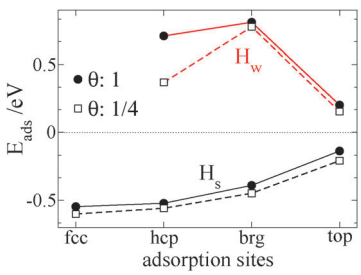

Fig. 4 Adsorption energies of the strongly and weakly adsorbed hydrogen (H_s and H_w respectively) on Rh(111) at different adsorption sites and coverages. The points for H_w are for a surface covered by a monolayer of H_s adsorbed in the fcc hollow sites.

For H_s the most favourable adsorption site is fcc hollow. Its large negative adsorption energy suggests that a monolayer of H_s is formed in such surfaces, as confirmed experimentally.[14,30] The energy decrease from $\theta = 1$ to $\theta = 1/4$ is due to the decrease of the H_s–H_s repulsion and is of the order of 0.1 eV. On this surface, covered with a monolayer of H_s at the fcc hollow sites, the adsorption of H_w takes place. In addition to the repulsion among H_s atoms, there are H_w–H_s repulsions which contribute to making $E_{ads}^{w} > E_{ads}^{s}$. In this case the top position is the most favourable one since there the latter force is the lowest.

2.3 Hydrogen adsorption on Rh/Au(111) and Rh/Pd(111) surfaces

The adsorption energies are calculated as in eqn (3) and (4) but now the index Subs refers to Rh/Au and Rh/Pd substrates. In Fig. 5, hydrogen adsorption energies as a function of the number of Rh overlayers (Rh_n) are shown. In order to determine the chemical effect of the gold or palladium substrates, we have proceeded as in our previous work[1] and also performed calculations for pure rhodium slabs expanded to the lattice constants of gold (Rh@Au) and palladium (Rh@Pd).

For the strongly adsorbed hydrogen, the first Rh overlayer is the most reactive one for both Rh/Pd and Rh/Au. There is still a minor chemical effect for the second layer, but from then on, the adsorption energies are almost the same as on the pure expanded Rh slabs (Rh@Au and Rh@Pd). From the second layer on, the change in the reactivity is mostly attributed to the lattice expansion. The adsorption energy on Rh_1/Au is ~0.42 eV lower than that on pure Rh(111), and is of the same order as on Pt(111).[35] For Rh_1/Pd the difference is smaller: ~0.18 eV. This suggests that Au induces a larger electronic effect on Rh than Pd, as will be confirmed later with density of states (DOS) studies. The adsorption energy on pure expanded Rh is ~0.16 eV and ~0.09 eV lower than on pure Rh for Rh@Au and Rh@Pd, respectively. This indicates that the geometric effect is also larger for Au than for Pd substrates which is expected since the lattice constant of Rh is expanded 8% and 4% correspondingly. The same trends were found for H_s at $\theta = 1/4$ (not shown) where an energy decrease of ~0.1 eV was obtained for all the adsorption sites computed.

For the weakly adsorbed hydrogen, and in contrast to the adsorption on pure Rh, E_{ads}^{w} is exothermic at the first Rh overlayer on both substrates (see Fig. 5b), which suggests that these structures are excellent catalysts for the HER. The electronic effect induced by the substrate extends only to the first Rh overlayer; for higher ones the geometric effect is dominant.

In order to study the electronic effect induced by Pd and Au substrates in greater detail, the DOS of the top Rh layer is illustrated in Fig. 6.

Comparing the first Rh overlayer in both substrates, it is clear that the upward shift of the *d*-band is larger on Rh_1/Au than on Rh_1/Pd. Also, a strong chemical effect is involved since the DOS of the overlayers are markedly different from those of the expanded lattices. Here this phenomenon follows the *d*-band model proposed by Hammer and Nørskov,[31,32] since this shift leads to an improvement of the chemisorption which is bigger for Rh/Au than for Rh/Pd overlayers. In order to make a quantitative comparison, the center of the *d*-band of pure Rh and of up to four Rh overlayers were calculated by means of eqn (5).

$$\int_{-\infty}^{\infty} \rho_d(\varepsilon)\varepsilon d\varepsilon = \varepsilon_d \qquad (5)$$

where $\rho_d(\varepsilon)$ is the DOS of the *d*-band as a function of the energy (ε). The results are shown in Fig. 7.

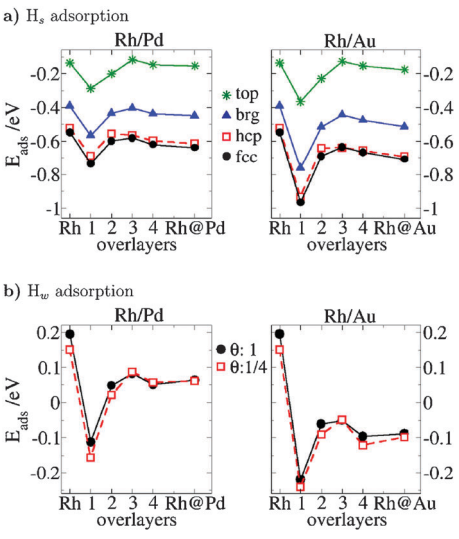

Fig. 5 (a) Adsorption energies (E_{ads}) of H_s at $\theta = 1$ on Rh_n/Pd and Rh_n/Au for $n = 1,2,\ldots,6$. (b) Adsorption energies of H_w at $\theta = 1$ and $\theta = 1/4$ on Rh_n/Pd and Rh_n/Au for $n = 1,2,\ldots,4$. (a–b) The values are compared with the adsorption energies on clean Rh(111) and on the laterally expanded slabs Rh@Pd and Rh@Au.

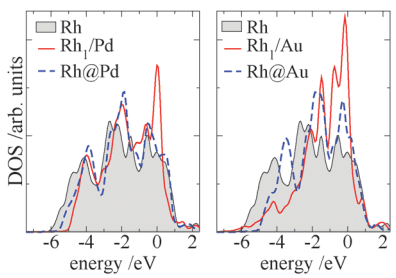

Fig. 6 Density of states (DOS) projected on the surface atoms of Rh, Rh/Pd and Rh/Au. The *d*-band states are plotted.

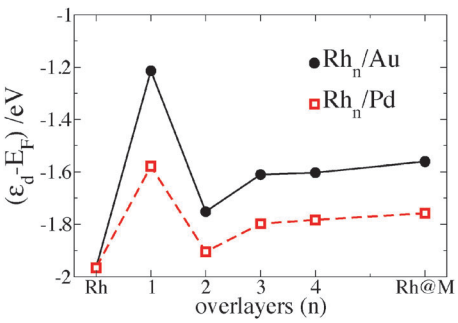

Fig. 7 Position ε_d of the *d*-band center with respect to the Fermi level as a function of the number of Rh overlayers on Au and on Pd substrates. The values are compared with the pure Rh surface (Rh) and the corresponding laterally expanded Rh (Rh@Sub).

It becomes evident that the electronic effect induced by the underlying substrate is larger for Au than for Pd. For both, after the second Rh overlayer the electronic effect contributes no longer to the *d*-band shift; it is then solely caused by the lattice expansion. Thus the situation is different than for Pd/Au(111) in different configurations, where the center of the d band does not correlate with the activity.[7]

3 Kinetics of the hydrogen reaction

3.1 The Volmer reaction

The DFT calculations have shown that the rhodium overlayers, particularly the monolayers, have a strong affinity for hydrogen, which makes them interesting candidates for catalysts. However, reaction rates are determined by activation barriers and only indirectly by thermodynamics. Therefore, we have investigated the first step of hydrogen evolution:

$$H^+ + e^- \rightarrow H_w, \qquad (6)$$

which is known as the Volmer reaction, by the theory of electrocatalysis developed in our group.[23] We focus on the activation energy at the standard hydrogen potential NHE, which is a good indicator of the reactivity. At this potential, the free energy for the Volmer reaction is given by the adsorption energies reported above plus an entropy term, which is of the order of 0.2 eV.[35] Thus, to obtain the free energies of adsorption at NHE a value of 0.2 eV has to be added. For a monolayer of Rh on Au(111) the free energy of adsorption for the weakly adsorbed species is −0.01 eV, and for Rh/Pd(111) it is 0.1 eV. So at NHE the Volmer reaction on both layers is almost isoenergetic, which in view of Sabatier's principle is favorable.

From our model for hydrogen evolution detailed in ref. 23, we have calculated the free energy surfaces for the Volmer reaction. Fig. 8 shows the result for Rh/Au(111). This plot shows the free energy of the system as a function of two coordinates: the solvent coordinate q and the distance from the surface. The former is a concept related to the Marcus theory[36] for electron transfer and characterizes the state of the solvent.

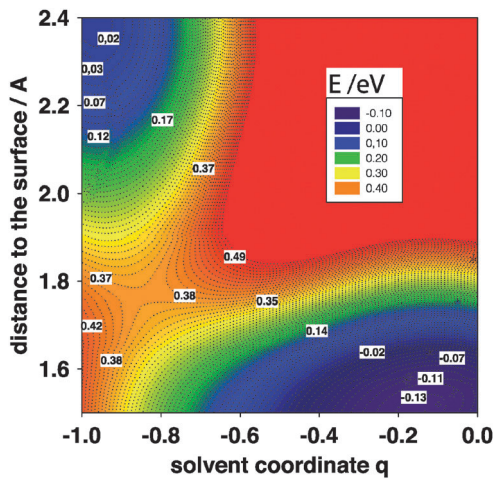

Fig. 8 Free energy surface for the Volmer reaction for H_w on a monolayer of Rh on Au(111) in the presence of a monolayer of H_s.

The transferring proton is strongly solvated, and its discharge requires a reorganization of the solvent. The solvent coordinate is defined in such a way, that a value of q indicates that the solvent would be in equilibrium with a reactant of charge $-q$.[37] Thus, the initial state is a proton at $q = -1$ and far from the surface, the final state an adsorbed hydrogen atom at $q = 0$ and on top. These two states are separated by an energy barrier of 0.37 eV, which is a very low value and of the same order of magnitude as for Pt(111)[21]—for comparison, for the coinage metals we have obtained barriers of about 0.7 eV. The surface for Rh/Pd(111) is very similar, and the energy of activation about 0.1 eV higher.

The position of the saddle point in Fig. 8 is noteworthy. Since the final state is adsorbed on top, the proton can approach the surface losing only a smaller part of its solvation sheath; therefore electron transfer occurs to a solvated state near $q \approx -0.85$. In contrast, when the final state is adsorbed in the fcc hollow site desolvation is stronger, and the saddle points, at NHE, are closer to $q = -0.5$.

3.2 H_2 dissociation on Rh(111) and Rh_1/Au(111) surfaces

The chemical recombination of two adsorbed hydrogen atoms (Tafel reaction) is often the second step in hydrogen evolution; on very active metals like Pt(111) and Re it determines the overall rate. It is simpler to discuss the results for the reverse reaction, the dissociation of H_2, since in this case the initial state is the same on all surfaces—a molecule far from the electrode. We have investigated this step both on pure Rh(111) and on a monolayer of Rh over Au(111), which is the better catalyst of our two monolayer systems. Since it does not involve electron transfer, it can be described by pure DFT.

Two types of surfaces were evaluated: a clean and a H_s-precovered surface. Details of the calculations are given in the appendix. In all cases, in the most favorable path the center of the H_s molecule is initially on top of a surface atoms, while the two atoms are close to the fcc and hcp hollow sites—we call this the f-t-h configuration (see Fig. 9).

Fig. 9 shows the potential energy of hydrogen dissociation as a function of the distance. On clean Rh or Rh_1/Au surfaces there is almost no activation barrier for the dissociation of hydrogen, which indicates that this process occurs instantaneously on these structures. Obviously, this is not the rate determining step for hydrogen evolution. As long as the dissociation proceeds, the surface coverage of H_s increases. Eventually, a hydrogen molecule will have no clean surface left to interact with. When the H_s monolayer is not complete, the dissociation of hydrogen is more favourable, but the barrier increases substantially as the H_s coverages grow.[21] In order to compare hydrogen dissociation on clean and covered surfaces, we investigated the limiting case, a complete H_s monolayer—see Fig. 9b.

At this H_s covered surface the incoming molecule has to overcome interatomic repulsion which significantly increases the activation energy. On Rh(111) this leads to a barrier of 0.88 eV, which is a little higher than that on Pt(111) under the same conditions.[21] Surprisingly, on Rh_1/Au the activation energy is only 0.16 eV. In the latter case, the barrier is comparable to that on clean Pt and Pd surfaces (0.06 eV[33] and 0.05 eV[34] correspondingly). The reasons for this dramatic difference can

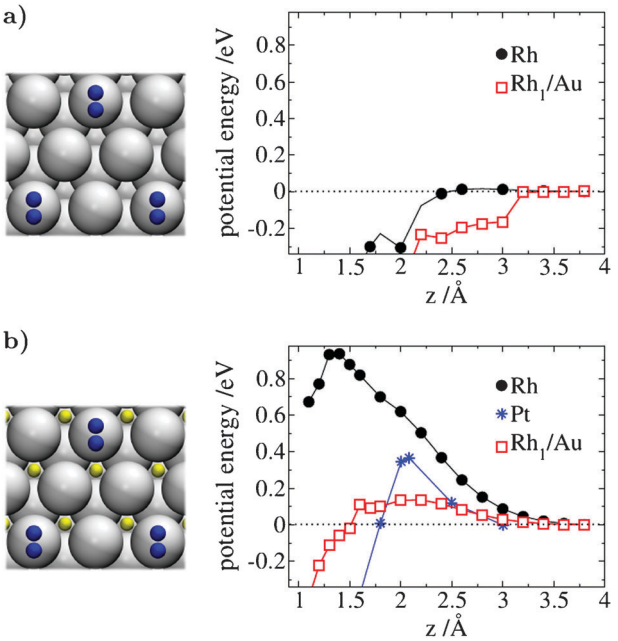

Fig. 9 Potential energy for the hydrogen dissociation process at different distances (z) from Rh and Rh_1/Au surfaces in the presence of a monolayer of H_s. The initial state of the f-t-h pathway is sketched at the left. (a) H_2 dissociation over a clean Rh and Rh_1/Au surface. (b) H_2 dissociation over a H_s-precovered surface of Rh and Rh_1/Au. For comparison, the corresponding curve for Pt(111) is also shown; this curve is for a coverage of 80% H_s, which roughly corresponds to the coverage at low overpotentials for hydrogen evolution.

be explained by two factors: the *repulsion* among hydrogen species and the *affinity* of the precovered surface for hydrogen adsorption.

Fig. 10a shows the initial state when a hydrogen molecule approaches a top site of a surface covered by a monolayer of H_s at fcc sites. As long as H_2 approaches the surface, the nuclear repulsion between the molecule and the H_s atoms is dominant and increases. This pushes the adsorbed atoms away from their fcc-hollow sites (see Fig. 10b), which also increases the repulsion among H_s neighbors sketched in Fig. 10a. The distance of two H_s neighbors (d_{H_s}) during the approach of a hydrogen molecule is shown in Fig. 10c. Since the lattice constant of Rh is smaller than that of gold, d_{H_s} is smaller for pure Rh surfaces, making the repulsion stronger than on Rh_1/Au. Indeed, the difference in d_{H_s} on these substrates is around 0.3 Å when H_2 is far from the substrate, and increases during its approach. The total hydrogen repulsion is the dominant force that increases the potential energy at distances larger than 2.5 Å. At closer distances, the molecule interaction with the substrate becomes stronger, and the affinity for hydrogen adsorption begins to play a role, and again, is quite different for both substrates. One way to compare them is by examining the bond distance of the molecule as it approaches the surface: the more favourable the interaction the sooner the H_2 bond distance increases. As shown in Fig. 10d, on Rh_1/Au the separation of the hydrogen molecule atoms occurs at larger distances from the surface than on Rh. Moreover, the elongation of the hydrogen bond is smooth on Rh_1/Au while in the case of Rh there is an abrupt change. At around 2.3 Å from the Rh_1/Au H_s-precovered surface the affinity for H_2 over-compensates hydrogen repulsion and consequently the energy of the system decreases (see Fig. 9b). The Rh H_s-precovered surface on the other hand has a weaker affinity for H_2 so that hydrogen repulsion dominates.

The differing affinities for H_2 of Rh and Rh_1/Au H_s-precovered surfaces can be analyzed with the aid of the DOS as shown in Fig. 11: at far distances from the surface H_2 shows a sharp peak which corresponds to the σ bonding state between the two atoms. At 2.2 Å from the surface only in the case of Rh_1/Au the molecule interacts with the substrate—principally with the s band, which extends further beyond the surface. At closer distances, on both surfaces hydrogen interacts with the s and the d band, both of which undergo significant changes. So, in the case of Rh_1/Au the electronic interaction with the metal starts at larger distances, and helps to reduce the activation barrier.

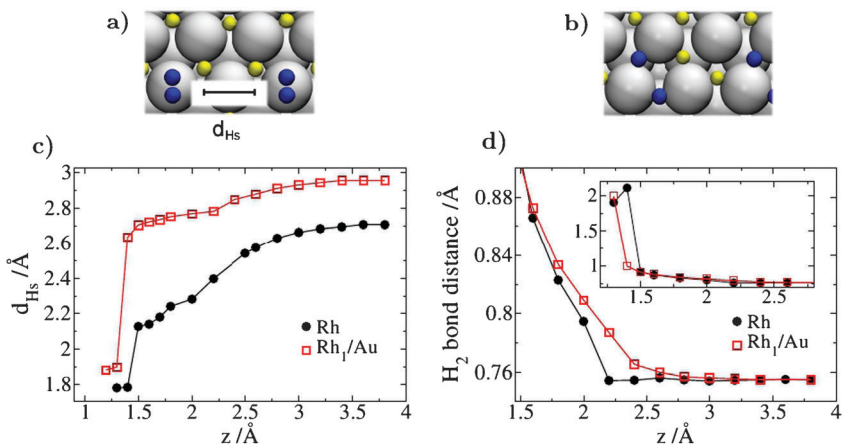

Fig. 10 (a) Top view of a H_s-precovered surface (yellow atoms) on which a H_2 molecule is approaching with the f-t-h configuration (blue atoms). The distance between two H_s atoms (d_{H_s}) is denoted with a segment within the figure. (b) Final state with the dissociated atoms. (c) d_{H_s} as a function of the distance from the hydrogen molecule to the surface (z). (d) H_2 bond distance as a function of z. The inset shows a zoomed view at shorter distances.

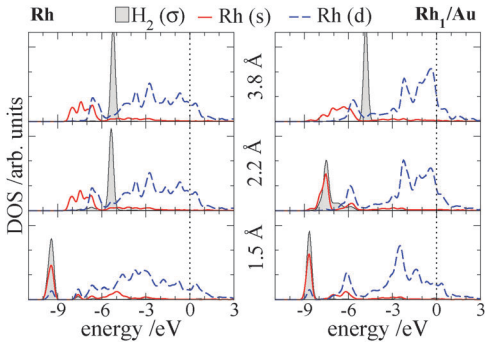

Fig. 11 Density of states (DOS) projected on the hydrogen molecule and surface metal atom states. Three stages of the H_2 dissociation on H_s-precovered surfaces are compared: H_2 far away from the surface (3.8 Å), closer (2.2 Å), and right before the molecule bond is broken (1.5 Å). The s state of hydrogen and Rh have been reduced by a factor of 4 for clarity.

4 Conclusions

Metal monolayers on foreign metal substrates have fascinating catalytic properties. They are only stable if there is a strong chemical bonding between the monolayer and the substrate, so there is always a pronounced chemical, or ligand, effect. If additionally the lattice constant of the adsorbed metal is smaller than that of the substrate, as is the case for Rh/Au(111) and Rh/Pd(111), the induced strain leads to an upward shift of the *d* band center of late transition metals, which increases the reactivity.

In the case of Rh/Au(111) the lattice mismatch is particularly large, and stable—or metastable—layers have only be observed in electrochemical systems. Hence, both the chemical and the strain effect are large, and combine to make this a very promising candidate for hydrogen electrocatalysis. According to our calculations, both hydrogen adsorption and recombination should be extremely fast, even faster than on pure Pt(111).

On Rh/Pd(111) the induced strain is weaker, so its catalytic properties are expected to be not quite as good. However, it should be more stable than Rh/Au(111).

To the best of our knowledge, there are no experimental investigations for hydrogen evolution or oxidation on these systems. Thus, our work is a prediction. This indicates a pronounced change in the relation between theory and experiment that has taken place during the last decade: Previously, theory used to follow the experimentalists trying to explain their data. Nowadays, experiments can be guided by theoretical predictions.

Appendix: computational details

First-principles calculations

All calculations were performed with DACAPO,[24] a density functional theory (DFT) code. The electron–ion interactions were accounted through ultrasoft pseudopotentials,[25] while the valence electrons were treated within the generalized gradient approximation (GGA) in the version of Perdew and Wang.[26,27] Special care was taken for the parametrization of the energy cutoff and the k-points sampling of the Brillouin zone based on the Monkhorst–Pack grid.[28] Both parameters were increased systematically until the change in the absolute energy was less than 10 meV. An energy cutoff of 450 eV and a grid of 8 × 8 × 1 satisfy the energy accuracy. For the relaxations computed, the convergence was achieved when the total forces were less than 0.01 eV $Å^{-1}$. Calculations with spin confirmed that the systems studied here are not magnetic.

Surface modeling

The lattice constants (a_0) were taken from the calculated equilibrium distances of a periodic fcc bulk: 3.83 Å for Rh, 3.99 Å for Pd and 4.18 Å for Au, which are in agreement with the experimental values[29] (3.80 Å, 3.88 and 4.07 Å respectively).

In order to choose the thickness of the monometallic slabs, the surface energy was calculated for several slabs of N layers by $\sigma = (E_{\mathrm{slab}(N)} - NE_{\mathrm{bulk}})/2$, where $E_{\mathrm{slab}(N)}$ is the energy of an N layer slab, and E_{bulk} is the energy per atom of the bulk. The surface energy difference between slabs of four and five layers is lower than 0.02 eV, therefore four layers were used for the rest of the calculations. The energy criterion of convergence was 0.02 eV, which is reached by a slab of four layers (Table 1).

Only the top two layers of the pure slabs were allowed to relax, and the bottom two were kept fixed in their corresponding bulk positions. Additional calculations with an expanded a_0 of pure Rh corresponding to Au (Rh@Au) and to Pd (Rh@Pd) were performed in order to study the effect of this expansion separately from the electronic effect induced by such substrates (Au or Pd). For Rh/Au and Rh/Pd slabs the structure was modeled by a four layers slab of the substrate, on which up to five layers of Rh were deposited. The bottom two layers of Pd or Au were kept fixed and the rest were fully relaxed. The same applied for the systems with hydrogen adsorbed at high symmetry sites. A vacuum corresponding to five layers was used in all systems.

Kinetics of the hydrogen reaction

The molecule was allowed to relax laterally on a plane parallel to and at different distances from the surface, whose first two layers were kept fixed. The rest was fully relaxed (including the hydrogen monolayer in the case of the precovered surface). The same procedure was used for the atomic hydrogen. For the latter case, the maximum hydrogen–surface distance computed was 2.4 Å, where the atom is non-magnetic. Thus, spin was not included.

The hydrogen molecule configurations are distinguished by three letters which indicate the position of the first hydrogen

Table 1 Surface energy (σ) with respect to the number of layers for Pd, Rh and Au fcc(111) surfaces

N	Pd σ/eV	Rh σ/eV	Au σ/eV
3	0.572	0.812	0.348
4	**0.559**	**0.824**	**0.350**
5	0.558	0.818	0.352
6	0.567	0.817	0.354
7	0.554	0.815	0.351

atom, the center of mass of the molecule, and the position of the second hydrogen atom, respectively, all with respect to the surface high symmetry sites: hcp-top-fcc (h-t-f), bridge-top-bridge (b-t-b), hcp-bridge-fcc (h-b-f) and top-bridge-top (t-b-t). The f-t-h configuration on clean and hydrogen covered surfaces is illustrated in Fig. 8.

Acknowledgements

Financial supports by the Deutsche Forschungsgemeinschaft (Schm 344/34-1,2, Sa 1770/1-1,2, and FOR 1376), by the European Union under COST and ELCAT, by an exchange agreement between the BMBF and CONICET, and by PICT-2008-0737 (ANPCyT) are gratefully acknowledged. E.S. and W.S. thank CONICET (PIP 11220100100411) for continued support. A generous grant of computing time from the Baden-Württemberg grid is gratefully acknowledged. E. N. Schulz thanks the DAAD for a stipend.

References

1 E. Santos, P. Quaino and W. Schmickler, *Electrochim. Acta*, 2010, **55**, 4346.
2 M. Gsell, P. Jakob and D. Menzel, *Science*, 1998, **280**, 5364.
3 P. Jakob, M. Gsell and D. Menzel, *J. Chem. Phys.*, 2001, **114**(22), 10075–10085.
4 S. Pandelov and U. Stimming, *Electrochim. Acta*, 2007, **52**(18), 5548–5555.
5 C. Köntje, L. Kibler and D. Kolb, *Electrochim. Acta*, 2009, **54**(14), 3830–3834.
6 J. Meier, K. A. Friedrich and U. Stimming, *Faraday Discuss.*, 2002, **121**, 365.
7 P. Quaino, E. Santos, H. Wolfschmidt, M. Montero and U. Stimming, *Catal. Today*, DOI: 10.1016/j.cattod.2011.05.004.
8 L. A. Kibler, M. Kleinert and D. M. Kolb, *J. Electroanal. Chem.*, 1999, **467**(1–2), 249–257.
9 J. Inukai and M. Ito, *J. Electroanal. Chem.*, 1993, **358**(1–2), 307–315.
10 G. A. Attard, R. Price and A. Al-Akl, *Surf. Sci.*, 1995, **335**, 52–62.
11 R. Gómez, A. Rodes, J. M. Pérez, J. M. Feliu and A. Aldaz, *Surf. Sci.*, 1995, **327**(3), 202–215.
12 R. Gómez, A. Rodes, J. M. Pérez, J. M. Feliu and A. Aldaz, *Surf. Sci.*, 1995, **344**(1–2), 85–97.
13 H. Yanagita, H. Fujioka, T. Aruga, N. Takagi and M. Nishijima, *Surf. Sci.*, 1999, **441**(2–3), 507–514.
14 S. Mann, T. Seto, C. Barnes and D. King, *Surf. Sci.*, 1992, **261**(1–3), 155–163.
15 S. Wilke, V. Natoli and M. H. Cohen, *J. Chem. Phys.*, 2000, **112**(22), 9986–9995.
16 See *e.g.* A. Groß, *Theoretical Surface Science*, Springer Verlag, Heidelberg, 2009, p. 255.
17 L. Vitas, A. V. Ruban, H. L. Skriver and J. Kollar, *Surf. Sci.*, 1998, **411**, 186.
18 E. I. Altman and R. J. Colton, *Surf. Sci. Lett.*, 1994, **304**, L406.
19 A. Michaelides, *Appl. Phys. A: Solid Surf.*, 2006, **85**, 415.
20 G. Jerkiewicz, *Prog. Surf. Sci.*, 1998, **57**(2), 137–186.
21 E. Santos, P. Hindelang, P. Quaino, E. N. Schulz, G. Soldano and W. Schmickler, *ChemPhysChem*, DOI: 10.1002/cphc.201100309.
22 E. Santos and W. Schmickler, *Angew. Chem., Int. Ed.*, 2007, **46**, 8262.
23 E. Santos, A. Lundin, K. Pötting, P. Quaino and W. Schmickler, *Phys. Rev. B: Condens. Matter Mater. Phys.*, 2009, **79**, 235436.
24 B. Hammer, L. B. Hansen and J. K. Nørskov, *Phys. Rev. B: Condens. Matter Mater. Phys.*, 1999, **59**(11), 7413–7421.
25 D. Vanderbilt, *Phys. Rev. B: Condens. Matter Mater. Phys.*, 1990, **41**(11), 7892–7895.
26 Y. Wang and J. P. Perdew, *Phys. Rev. B: Condens. Matter Mater. Phys.*, 1991, **44**(24), 13298–13307.
27 J. P. Perdew, J. A. Chevary, S. H. Vosko, K. A. Jackson, M. R. Pederson, D. J. Singh and C. Fiolhais, *Phys. Rev. B: Condens. Matter Mater. Phys.*, 1992, **46**(11), 6671–6687.
28 J. H. Monkhorst and D. J. Pack, *Phys. Rev. B: Solid State*, 1976, **13**(12), 5188–5192.
29 C. Kittel, in: *Introduction to Solid States Physics*, 8th edn, Wiley & Sons, 2005, p. 20.
30 J. I. Colonell, T. J. Curtiss and S. J. Sibener, *Surf. Sci.*, 1996, **366**(1), 19–28.
31 B. Hammer and J. K. Nørskov, *Surf. Sci.*, 1995, **343**(3), 211–220.
32 B. Hammer and J. K. Nørskov, *Nature*, 1995, **376**, 238–240.
33 N. B. Arboleda and H. Kasai, *Surf. Interface Anal.*, 2008, **40**(6–7), 1103–1107.
34 C. Resch, H. Berger, K. Rendulic and E. Bertel, *Surf. Sci.*, 1994, **316**(3), L1105–L1109.
35 J. K. Norskøv, T. Bligaard, A. Logadottir, J. R. Kitchin, J. G. Chen, S. Pandelov and U. Stimming, *J. Electrochem. Soc.*, 2005, **152**, J23.
36 R. A. Marcus, *J. Chem. Phys.*, 1956, **24**, 966.
37 W. Schmickler and E. Santos, *Interfacial Electrochemistry*, Springer, Heidelberg, 2010, ch. 10.